Volume 56
Number 35
2 May 2020
Pages 4739–4860

ChemComm

Chemical Communications

rsc.li/chemcomm

ISSN 1359-7345

ROYAL SOCIETY OF CHEMISTRY

COMMUNICATION

Bernd M. Schmidt *et al.*

A porous fluorinated organic [4+4] imine cage showing CO_2 and H_2 adsorption

ChemComm

ROYAL SOCIETY OF CHEMISTRY

COMMUNICATION

View Article Online
View Journal | View Issue

Cite this: *Chem. Commun.*, 2020, **56**, 4761

Received 11th March 2020,
Accepted 31st March 2020

DOI: 10.1039/d0cc01872d

rsc.li/chemcomm

A porous fluorinated organic [4+4] imine cage showing CO_2 and H_2 adsorption†

Tom Kunde, [a] Esther Nieland, [a] Hendrik V. Schröder, ‡[b] Christoph A. Schalley [b] and Bernd M. Schmidt *[a]

We present the synthesis of a porous, organic [4+4] imine cage containing perfluorinated aromatic panels. Gas adsorption experiments show an uptake of 19.0 wt% CO_2 (4.2 mmol g^{-1}, 273 K and at 1 bar) and 1.5 wt% H_2 (7.5 mmol g^{-1}, 77 K and at 1 bar) for the specific surface area of 536 m^2 g^{-1} of the crystalline material obtained directly from the reaction mixture, combined with an outstanding thermal stability, making it a very interesting porous material suitable for gas adsorption.

Fluorinated and perfluorinated molecules have been extensively reviewed in comparison to their hydrogenated counterparts. Besides widespread incorporation into pharmaceuticals, especially fluorinated polymers show desirable material properties such as high thermal and chemical stability, making fluorine-containing molecules important for life science[1] and material applications.[2] Together with metal–organic (MOFs)[3] and covalent organic (COFs)[4] frameworks, fluorinated metal–organic frameworks (FMOFs) are characterised by a highly modular synthesis with excellent properties in regards to thermal stability, catalytic activity, high gas affinity and selectivity.[5] The groups of Omary and Miljanić reported ultra-hydrophobic FMOFs that show promising gas adsorption capabilities and a high capacity and affinity to hydrocarbons.[6] In addition, the group of Miljanić could show that their highly fluorinated tetrazolate-based MOF exhibits exceptionally high uptake capabilities for ozone-depleting fluorocarbons and chlorofluorocarbons (CFCs).[6b] Fluorinated metal-free COFs were for example reported by the groups of Jiang and Cooper, showing a higher crystallinity and gas uptake in comparison to their non-fluorinated counterparts.[7,8] Remarkable accessible surface areas of up to 1821 m^2 g^{-1} were reported for non-covalent organic frameworks/porous molecular crystals that can effectively adsorb hydrocarbons, CFCs and fluorinated anaesthetics.[9] Porous organic cages (POCs) are discrete, three-dimensional molecular assemblies that unlike networks, allow for straightforward processing and analysis in solution.[10] The most thoroughly investigated class of porous [4+6] imine cages originates from the group of Cooper, forming crystalline porous materials, porous liquids and POC nanocrystals or core–shell crystals depending on functionalization and processing.[10,11] To our surprise, only very few fluorinated POCs have been reported.[12]

First reports indicated that the influence of cage building blocks with a low fluorination grade does not have a beneficial effect on the material properties like gas adsorption and crystal packing.[12a,c] However, reports on MOFs and COFs demonstrate that tuning the electronic properties of the intrinsic pore by very electron withdrawing and hydrophobic fluorine substituents often improves performance.[6] Herein, we report a novel fluorinated [4+4] imine cage (**FC1**). **FC1** is synthesised by imine condensation of 1,3,5-triformylbenzene (**1**) and 1,3,5-tris(aminomethyl)-2,4,6-trifluorobenzene (**2**) (Fig. 1a). Mixing the two building blocks in a 1 : 1 stoichiometry in dichloromethane/methanol (3 : 1) without stirring yields needle-like crystals in 67% yield over the course of two days at room temperature. NMR analysis of the redissolved crystals shows sharp signals both in the ^{1}H as well as in the ^{19}F NMR (Fig. 1c), which indicates clean cage crystallisation without polymeric side product precipitation. DOSY experiments reveal an approximate hydrodynamic radius of r_{solv} = 0.71 nm (D = 5.5 × 10^{-10} m^2 s^{-1} in $CDCl_3$, Fig. S1, ESI†). Unusual for supramolecular cage building blocks, both **1** and **2** are rather flexible structures in which the functional groups are not sterically constrained in a specific orientation.[10a] The common strategy to synthesise a self-assembled cage compound, whether metal–organic or organic, is largely dependent on the degree of preorganization in at least one of the ligands.[4e] We calculated the rotational barrier of **2** to be 7 kcal mol^{-1} (MM2, rotation around the C1–C2-bond, see Fig. 1a). This is significantly lower than the barrier of the commonly employed 1,3,5-tris(aminomethyl)-2,4,6-triethyl-benzene

[a] *Institut für Organische Chemie und Makromolekulare Chemie, Heinrich-Heine-Universität Düsseldorf, Universitätsstraße 1, D-40225 Düsseldorf, Germany. E-mail: Bernd.Schmidt@hhu.de*
[b] *Institut für Chemie und Biochemie, Freie Universität Berlin, Arnimallee 20, D-14195 Berlin, Germany*

† Electronic supplementary information (ESI) available: Synthetic methods, analytical data, X-ray crystallographic details and additional data. See DOI: 10.1039/d0cc01872d

‡ Present address: Department of Chemical and Biological Engineering, Princeton University, Princeton, NJ 08544, USA.

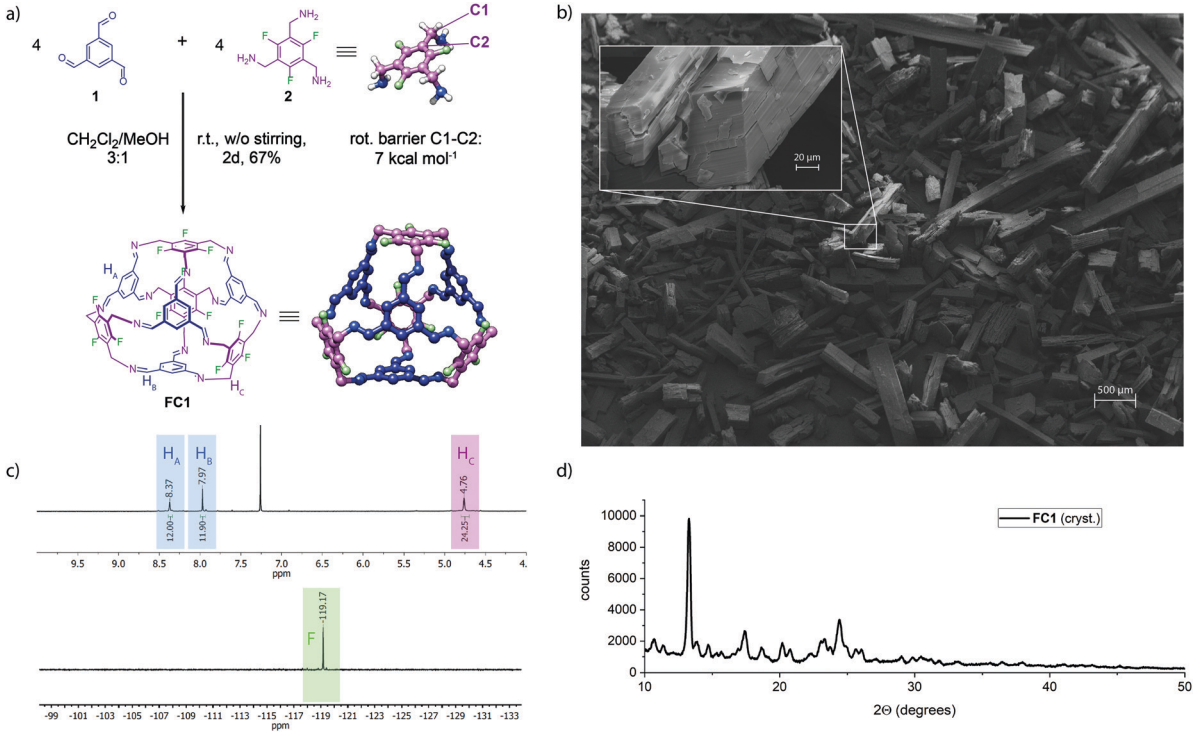

Fig. 1 (a) Synthesis of **FC1** by combining equal amounts of **1** and **2** in dichloromethane/methanol 3 : 1 at room temperature; the molecular structure of triamine **2**, as obtained from calculations using hybrid B3LYP 6-311++G(d,p) level of theory, showing the possible preorganization by weak C–H···F contacts and the rotational barrier of the amines obtained from MM2 calculations; the calculated structure of the truncated tetrahedral cage **FC1** (M062X/def2-TZVP); (b) scanning electron microscope (SEM) image of crystalline **FC1**, scanning voltage 12 kV; (c) ^{1}H and ^{19}F NMR of the precipitated crystalline material, in $CDCl_3$ at 25 °C; (d) experimental powder X-ray diffraction (XRD) pattern of crystalline **FC1**, for a comparison of crystalline and calculated powder XRD patterns, see Fig. S12 (ESI†).

(227.7 kcal mol^{-1}, see Fig. S4 and S5, ESI†),[13b] which is often chosen because of the all-*cis* orientation of the amino groups. The successful synthesis of **FC1** in very good yields of 67% as a crystalline material, despite the low rotational barrier in **2**, might be explained by the minute electronic effects of the fluorine substituents and not by pure sterical congestion. When Mastalerz *et al.* reported similar truncated tetrahedral [4+4] POCs in 2018, they did not observe formation of imine cages when using non-bulky substituents, instead polymeric structures were formed.[13] Our imine cage **FC1** forms rather quickly under the given conditions and precipitates cleanly.

Powder XRD of precipitated **FC1** shows sharp reflexes, indicating a highly crystalline and homogeneous material (Fig. 1d). SEM images further support this claim, showing only up to 100 µm thick, long needle-like crystals (Fig. 1b). Thermogravimetric analysis shows that fluorinated imine cage **FC1** is also highly stable. The decomposition temperature of 373 °C is significantly higher than of non-fluorinated imine cages of similar size (300 °C).[13b,14] A model of **FC1** obtained from DFT calculations using M062X/def2-TZVP basis set indicates a spherical intrinsic pore with a diameter of about 6.4 Å (Fig. 2a). Analysis of the calculated structure using pywindow[15] reveals the six pore-windows to be of about 3.4 Å in diameter (X-ray structural data was only used to confirm the connectivity of the pores within the network). Derived from the ideal model, the desolvated cage cavity should be in principle accessible to gases like N_2 and H_2. After filtering off the needle-like crystals of **FC1** from the reaction mixture, the crystals were dried and degassed at 80 °C for 16 hours, prior to gas adsorption experiments. The specific surface area for the crystalline material of 536 m^2 g^{-1} (derived from the Brunauer–Emmett–Teller (BET) isotherm) is comparable to the similarly sized propanediamine **CC2** cage (SA_{BET} = 533 m^2 g^{-1}) reported by Cooper *et al.*, while the values of the cyclohexanediamine **CC3** POC (SA_{BET} = 624 m^2 g^{-1}) are slightly higher.[11d] The corresponding isotherm of **FC1** agrees very well with a microporous type I model (Fig. 2b). **FC1** shows a 1.5 times higher uptake of up to 19.0 wt% CO_2 (4.2 mmol g^{-1}, 273 K and at 1 bar) and 1.5 wt% H_2 (7.5 mmol g^{-1}, 77 K and at 1 bar) compared to similar sized **CC2** (13.2 wt% CO_2, 1.2 wt% H_2) and **CC3** (11.0 wt% CO_2, 1.0 wt% H_2).[12d] An explanation for the higher gas uptake is likely found in the higher hydrophobicity inside the cavity due to the fluorinated aromatic panels of Janus-like **FC1**. Recent studies of Miljanić *et al.* also suggest that fluorination increases CO_2-philicity, as shown by comparing perfluorinated and non-fluorinated covalent triazine frameworks (CTFs) of almost identical surface area.[6a]

A high BET surface area of POCs usually results from efficient window-to-window packing.[12a] To further understand the adsorption behaviour, it is necessary to consider the pore connectivity within the material, usually available from single-crystal X-ray data. Although **FC1** readily crystallizes from methanol/chloroform mixtures, a data set suitable for initial refinement in

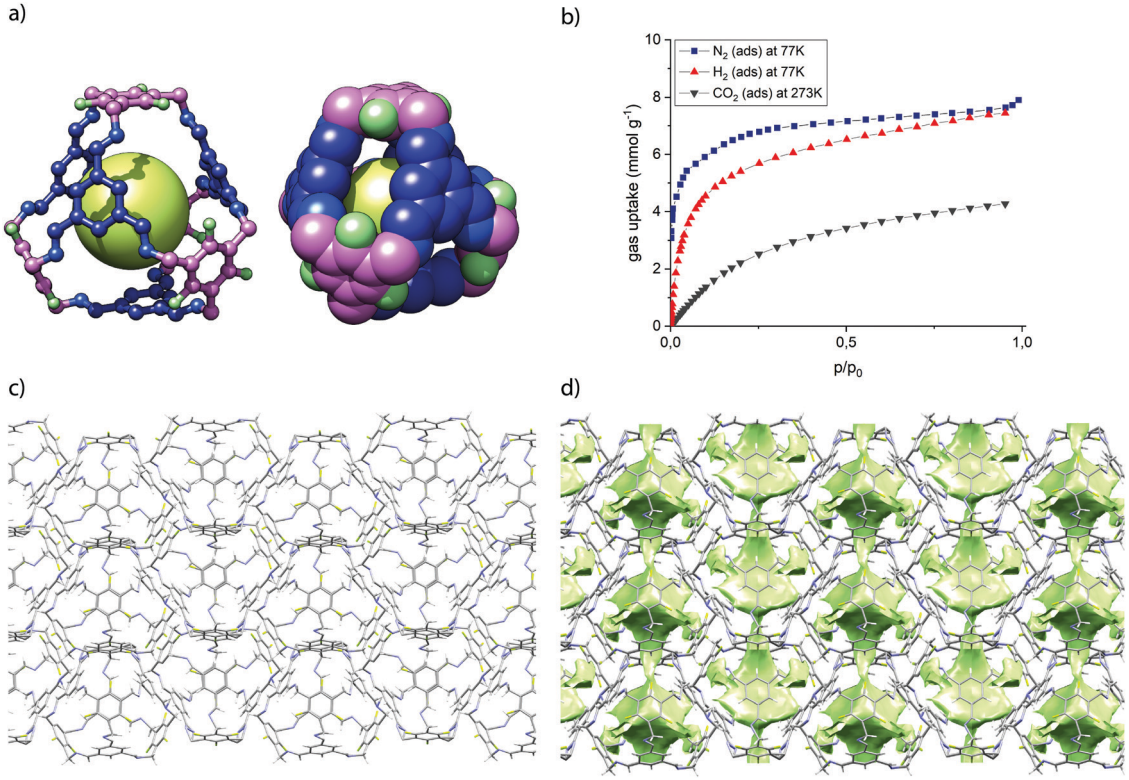

Fig. 2 (a) Calculated structure of **FC1** (M062X/def2-TZVP, ball-and-stick model left and space-filling model right) together with the calculated spherical pore (volume of 158.2 Å^3, green) using pywindow;[18] (b) gas adsorption isotherms for N_2 at 77 K (blue), H_2 at 77 K (red) and CO_2 at 273 K (grey); (c) crystal packing of **FC1** as obtained from the single-crystal structure, disordered solvent molecules within the pores were omitted for clarity; (d) solvent accessible surface area without solvents for a molecular probe with 1.2 Å radius (green) within the crystal lattice. Due to the disorder is in the solid state, all calculations regarding intrinsic porosity were conducted using the ideal DFT geometry.

the monoclinic space group $P2_1$ of the heavily solvated structures was measured at DESY's synchrotron diffraction beamline P11 at PETRA III with a 0.9 Å resolution and is shown in the ESI† (Fig. S9–S11). Looking along the crystallographic *a* axis, an infinite channel is constructed by window-to-window packing of **FC1** cages (Fig. 2c, d and Fig. S11, ESI†). These results are in excellent agreement with the high BET surface area observed. Because no bulky substituents are gating the pores, accessibility is similarly high for all of the gases studied herein. These results prove that highly fluorinated POCs share to some extent the very hydrophobic nature of fluorinated MOFs and are a promising lead to new gas separation and storage materials.

MALDI as well as electrospray ionization (ESI) mass spectra showed peaks for protonated dimers of **FC1**. Recent reports of interlocked covalent organic cages, motivated us to investigate, whether our samples of **FC1** contain significant amounts of potentially sparingly soluble interlocked species.[16] In order to test whether these ions might correspond to interlocked species, collision-induced dissociation (CID) experiments were performed. Structure-indicative fragments generated by CID can be subsequently analysed with ion mobility-mass spectrometry.[17] A sample of a chloroform/acetonitrile (9 : 1) solution of **FC1** was ionized by ESI. The weak signal corresponding to the $[2M + H]^+$ ion (*m*/*z* 2618) was mass-selected and subjected to CID, alongside the monomolecular $[M + H]^+$ as a reference, applying different collision voltages. At 60 V we found a series of fragmented ions (see Fig. S13b, ESI†). The clean dissociation of $[2M + H]^+$ ions into a neutral and a protonated cage at already 20 V, however, clearly speaks against catenation and these ions thus represent proton-bridged dimers that form during ionization (Fig. S14b, ESI†).

Considering the Janus-like (''two-faced'') surface of **FC1** having an alternating series of electron-deficient and electron-rich aromatic panels, we investigated the possibility of **FC1** to form host–guest complexes with different aromatic molecules. A solution of **FC1** with an excess of each aromatic guest was sonicated and analysed by ESI-MS (Fig. S16 and Table S3, ESI†). To our surprise, only electron-deficient benzonitrile, hexafluorobenzene and *para*-iodo-nitrobenzene were able to form strong enough host–guest complexes that survive the electrospray ionization process without complete dissociation. Another CID experiment with the mass-selected **FC1**-benzonitrile complex (*m*/*z* 1412) clearly confirmed its non-covalent nature (Fig. S17, ESI†). Since **FC1** is able to form complexes in the gas phase, we also briefly looked into the binding behaviour in solution as well. A solution of **FC1** in $CDCl_3$ was titrated with 1 and 10 equiv. of benzonitrile and hexafluorobenzene and the corresponding shift in ^{1}H and ^{19}F NMR was recorded. However, no complexation-induced chemical shift changes were observed. To increase binding, we reduced the imine bonds of **FC1**, effectively 'locking' the cage.[10] The generated amine

cage $\mathbf{FC1_L}$ was mixed with an excess of the aromatic guests in a H_2O/iPrOH/HCOOH (50 : 50 : 1) solution and was then again subjected to ESI-MS experiments. However, no host–guest complexes were observed (Fig. S18 and Table S3, ESI†), which is consistent with reports showing increased flexibility within amine cages, accompanied by collapsed cavities (and loss of porosity in the solid state).[11b]

We herein reported the synthesis and characterisation of the first POC, containing perfluorinated aromatic panels. **FC1** forms quickly and in high purity, despite low preorganization encoded in the starting materials. The POC was investigated in terms of classic host–guest chemistry in solution and in the gas phase. While **FC1** forms strong non-covalent adducts with electron-deficient aromatics in MS experiments, it is a poor host in solution, unchanged by reduction to amine $\mathbf{FC1_L}$. However, [4+4] imine cage **FC1** shows outstanding thermal and adsorption properties in the solid state, because of infinite channels connecting the tetrahedral pores. Our reported H_2 and CO_2 uptakes are amongst the highest reported for similar-sized POCs, which makes **FC1** a promising candidate for the use in gas storage and separation materials. The cage thus indeed shows Janus-like behaviour. In the solid state, the fluorinated aromatic panels increases CO_2-philicity, in the gas phase however, host–guest interactions to the non-fluorinated panels seem preferable.

We thank N. Nöthling, R. Goddard, C. W. Lehmann and the team at DESY's P11 beamline. This work was supported by the Fonds der chemischen Industrie (Kekulé fellowship, T. K.), the Strategic Research Fund of Heinrich Heine University (F-2018/1460-4) and the Deutsche Forschungsgemeinschaft (387284271 – SFB 1349). Support with ESI-MS experiments from the BioSupraMol core facility at FU Berlin is gratefully acknowledged.

Conflicts of interest

There are no conflicts to declare.

References

1 H. J. Böhm, D. Banner, S. Bendels, M. Kansy, B. Kuhn, K. Müller, U. Obst-Sander and M. Stahl, *ChemBioChem*, 2004, **5**, 637.
2 (*a*) L. Hou, X. Zhang, G. F. Cotella, G. Carnicella, M. Herder, B. M. Schmidt, M. Pätzel, S. Hecht, F. Cacialli and P. Samorì, *Nat. Nanotechnol.*, 2019, **14**, 347; (*b*) F. Babudri, G. M. Farinola, F. Naso and R. Ragni, *Chem. Commun.*, 2007, 1003; (*c*) K. Reichenbächer, H. I. Süss and J. Hulliger, *Chem. Soc. Rev.*, 2005, **34**, 22.
3 (*a*) A. Schneemann, V. Bon, I. Schwedler, I. Senkovska, S. Kaskel and R. A. Fischer, *Chem. Soc. Rev.*, 2014, **43**, 6062; (*b*) H. Furukawa, K. E. Cordova, M. O'Keeffe and O. M. Yaghi, *Science*, 2013, **341**, 1230444; (*c*) H.-C. Zhou, J. R. Long and O. M. Yaghi, *Chem. Rev.*, 2012, **112**(2), 673; (*d*) N. L. Rosi, J. Eckert, M. Eddaoudi, D. T. Vodak, J. Kim, M. O'Keeffe and O. M. Yaghi, *Science*, 2003, **300**, 1127; (*e*) S. L. James, *Chem. Soc. Rev.*, 2003, **32**, 276.
4 (*a*) S. Klotzbach and F. Beuerle, *Angew. Chem., Int. Ed.*, 2015, **54**, 10356; (*b*) A. Dhara and F. Beuerle, *Chem. – Eur. J.*, 2015, **21**, 17391; (*c*) S. Klotzbach, T. Scherpf and F. Beuerle, *Chem. Commun.*, 2014, **50**, 12454; (*d*) C. J. Doonan, D. J. Tranchemontagne, T. G. Glover, J. R. Hunt and O. M. Yaghi, *Nat. Chem.*, 2010, **2**, 235; for recent reviews see: (*e*) F. Beuerle and B. Gole, *Angew. Chem., Int. Ed.*, 2018, **57**, 4850; (*f*) S.-Y. Ding and W. Wang, *Chem. Soc. Rev.*, 2013, **42**, 548.
5 (*a*) Z. Zhang and O. Š. Miljanić, *Org. Mat.*, 2019, **1**, 19; (*b*) S.-I. Noro and T. Nakamura, *NPG Asia Mater.*, 2017, **9**, e433.
6 (*a*) Z. Yang, S. Wang, Z. Zhang, W. Guo, K. Jie, M. I. Hashim, O. Š. Miljanić, D.-E. Jiang, I. Popovs and S. Dai, *J. Mater. Chem. A*, 2019, **7**, 17277; (*b*) T.-H. Chen, I. Popov, W. Kaveevivitchai, Y.-C. Chuang, Y.-S. Chen, A. J. Jacobson and O. Š. Miljanić, *Angew. Chem., Int. Ed.*, 2015, **54**, 13902; (*c*) T.-H. Chen, I. Popov, O. Zenasni, O. Daugulis and O. Š. Miljanić, *Chem. Commun.*, 2013, **49**, 6846; (*d*) C. Yang, U. Kaipa, Q. Z. Mather, X. Wang, V. Nesterov, A. F. Venero and M. A. Omary, *J. Am. Chem. Soc.*, 2011, **133**, 18094; (*e*) C. Yang, X. Wang and M. A. Omary, *Angew. Chem., Int. Ed.*, 2009, **48**, 2500.
7 X. Chen, M. Addicoat, S. Irle, A. Nagai and D. Jiang, *J. Am. Chem. Soc.*, 2013, **135**, 546.
8 R. Dawson, A. Laybourn, R. Clowes, Y. Z. Khimyak, D. J. Adams and A. I. Cooper, *Macromolecules*, 2009, **42**, 8809.
9 (*a*) M. I. Hashim, H. T. M. Le, T. H. Chen, Y. S. Chen, O. Daugulis, C. W. Hsu, A. J. Jacobson, W. Kaveevivitchai, X. Liang, T. Makarenko, O. S. Miljanic, I. Popovs, H. V. Tran, X. Wang, C. H. Wu and J. I. Wu, *J. Am. Chem. Soc.*, 2018, **140**, 6014; (*b*) T.-H. Chen, W. Kaveevivitchai, A. J. Jacobson and O. Š. Miljanić, *Chem. Commun.*, 2015, **51**, 14096; (*c*) T.-H. Chen, I. Popov, W. Kaveevivitchai, Y.-C. Chuang, Y.-S. Chen, O. Daugulis, A. J. Jacobson and O. Š. Miljanić, *Nat. Commun.*, 2014, **5**, 5131.
10 (*a*) M. Mastalerz, *Acc. Chem. Res.*, 2018, **51**, 2411; (*b*) M. E. Briggs and A. I. Cooper, *Chem. Mater.*, 2017, **29**, 149; (*c*) T. Hasell and A. I. Cooper, *Nat. Rev. Mater.*, 2016, **1**, 16053; (*d*) G. Zhang and M. Mastalerz, *Chem. Soc. Rev.*, 2014, **43**, 1934.
11 (*a*) S. Jiang, Y. Du, M. Marcello, E. W. Corcoran, Jr., D. C. Calabro, S. Y. Chong, L. Chen, R. Clowes, T. Hasell and A. I. Cooper, *Angew. Chem., Int. Ed.*, 2018, **57**, 11228; (*b*) M. Liu, M. A. Little, K. E. Jelfs, J. T. Jones, M. Schmidtmann, S. Y. Chong, T. Hasell and A. I. Cooper, *J. Am. Chem. Soc.*, 2014, **136**, 7583; (*c*) T. Hasell, S. Y. Chong, K. E. Jelfs, D. J. Adams and A. I. Cooper, *J. Am. Chem. Soc.*, 2012, **134**, 588; (*d*) T. Tozawa, J. T. Jones, S. I. Swamy, S. Jiang, D. J. Adams, S. Shakespeare, R. Clowes, D. Bradshaw, T. Hasell, S. Y. Chong, C. Tang, S. Thompson, J. Parker, A. Trewin, J. Bacsa, A. M. Slawin, A. Steine and A. I. Cooper, *Nat. Mater.*, 2009, **8**, 973.
12 (*a*) S. M. Elbert, N. I. Regenauer, D. Schindler, W. S. Zhang, F. Rominger, R. R. Schroder and M. Mastalerz, *Chem. – Eur. J.*, 2018, **24**, 11438; (*b*) T. Jiao, L. Chen, D. Yang, X. Li, G. Wu, P. Zeng, A. Zhou, Q. Yin, Y. Pan, B. Wu, X. Hong, X. Kong, V. M. Lynch, J. L. Sessler and H. Li, *Angew. Chem., Int. Ed.*, 2017, **56**, 14545; (*c*) M. J. Bojdys, M. E. Briggs, J. T. A. Jones, D. J. Adams, S. Y. Chong, M. Schmidtmann and A. I. Cooper, *J. Am. Chem. Soc.*, 2011, **133**, 16566; (*d*) H. Plenio and R. Diodone, *Z. Naturforsch., B: J. Chem. Sci.*, 1995, **50b**, 1075.
13 (*a*) J. C. Lauer, Z. Pang, P. Janßen, F. Rominger, T. Kirschbaum, M. Elstner and M. Mastalerz, *ChemistryOpen*, 2020, **9**, 183; (*b*) J. C. Lauer, W. S. Zhang, F. Rominger, R. R. Schroder and M. Mastalerz, *Chem. – Eur. J.*, 2018, **24**, 1816.
14 (*a*) N. Giri, C. E. Davidson, G. Melaugh, M. G. Del Pópolo, J. T. Jones, T. Hasell, A. I. Cooper, P. N. Horton, M. B. Hursthouse and S. L. James, *Chem. Sci.*, 2012, **3**, 2153; (*b*) T. Hasell, M. Schmidtmann and A. I. Cooper, *J. Am. Chem. Soc.*, 2011, **133**, 14920.
15 M. Miklitz and K. E. Jelfs, *J. Chem. Inf. Model.*, 2018, **58**, 2387.
16 (*a*) G. Zhang, O. Presly, F. White, I. M. Oppel and M. Mastalerz, *Angew. Chem., Int. Ed.*, 2014, **53**, 5126; (*b*) T. Hasell, X. Wu, J. T. Jones, J. Bacsa, A. Steiner, T. Mitra, A. Trewin, D. J. Adams and A. I. Cooper, *Nat. Chem.*, 2010, **2**, 750.
17 (*a*) A. Kruve, K. Caprice, R. Lavendomme, J. M. Wollschläger, S. Schoder, H. V. Schröder, J. R. Nitschke, F. B. L. Cougnon and C. A. Schalley, *Angew. Chem., Int. Ed.*, 2019, **58**, 11324; (*b*) K. Caprice, M. Pupier, A. Kruve, C. A. Schalley and F. B. L. Cougnon, *Chem. Sci.*, 2018, **9**, 1317; (*c*) U. Warzok, M. Marianski, W. Hoffmann, L. Turunen, K. Rissanen, K. Pagel and C. A. Schalley, *Chem. Sci.*, 2018, **9**, 8343.

